

Scaling law for three-body collisions near a narrow s -wave Feshbach resonance

Jiaming Li,^{1,2,3,*} Shuai Peng,¹ Yirou Xu,¹ Shiyin Kuang,¹ and Le Luo^{1,2,3,4,†}

¹*School of Physics and Astronomy, Sun Yat-Sen University, Zhuhai, Guangdong, China 519082*

²*Center of Quantum Information Technology, Shenzhen Research Institute of Sun Yat-sen University, Shenzhen, Guangdong, China 518087*

³*State Key Laboratory of Optoelectronic Materials and Technologies,
Sun Yat-Sen University, Guangzhou, Guangdong, China 510275*

⁴*Quantum Science Center of Guangdong-Hongkong-Macao Greater Bay Area, Shenzhen, Guangdong, China 518048*

(Dated: October 24, 2023)

Ultracold atomic gases provide a controllable system to study the inelastic processes for three-body systems, where the three-body recombination rate depends on the scattering length scaling. Such scalings have been confirmed in bosonic systems with various interaction strengths, but their existence with fermionic atoms remains elusive. In this work, we report on an experimental investigation of the scaling law for the three-body atomic loss rate L_3 in a two-component ${}^6\text{Li}$ Fermi gas with the scattering length $a < 0$. The scaling law is validated within a certain range of a near the narrow s -wave Feshbach resonance, where $L_3 \propto T|a|^{2.60(5)}$, and T is the gas temperature. The scaling law is observed to have an upper and a lower bound in terms of the scattering length. For the upper bound, when $a \rightarrow \infty$, the power-law scaling is suppressed by the unitary behavior of the resonance caused by the strong three-body collisions. For the lower bound, $a \rightarrow 0$, the finite range effect modifies the scaling law by the effective scattering length L_e . These results indicate that the three-body recombination rate in a fermionic system could be characterized by the scaling law associated with the generalized Efimov physics.

Studies of quantum three-body physics help to clarify some fundamental properties of a many-body system, ranging from the formation of the first star [1] to the exotic nuclear dynamics [2]. However, being immersed in a real system with many-particles, the three-body process is usually difficult to be solved in an analytical way. In past decades, ultracold quantum gases have provided an ideal experimental platform for quantitatively studying few-body physics, indebted to the precise-tuned interaction via Feshbach resonances [3–10]. As a notable example, the dependence of the three-body loss rate L_3 on the two-body scattering length a attracted substantial attention [11–15].

The $L_3 \propto a^4$ scaling of three identical bosons have been theoretically predicted and experimentally confirmed in both $a > 0$ and $a < 0$ regions [16–18]. For identical fermions, their L_3 relates to the p -wave scattering volume V_p has been predicted to scale as $V_p^{8/3}$ when $V_p < 0$ [19], which was also confirmed in the experiment of a single-spin component ${}^6\text{Li}$ fermi gas [20]. For a two-component Fermi gas with the s -wave interaction, a weakly bound molecule is formed in the $a > 0$ regime where the predicted $L_3 \propto a^6$ was verified recently using a homogeneous gas with a box trapping potential in the Bose-Einstein condensation (BEC) side of the broad Feshbach resonance of ${}^6\text{Li}$ [21, 22].

On the other hand, the scaling law in the Bardeen-Cooper-Schrieffer (BCS) side, $a < 0$, has yet to be well understood. So far, in the BCS side, L_3 has been observed scaling as $|a|^{0.79(14)}$ in a quasi-two-dimensional Fermi gas [23], which is quite different from the theoretical prediction of $|a|^{2.455}$ basing on the adiabatic hyperspherical representation with an effective three-body repulsive potential [24]. Very recently, Ref. [25] proposes that the p -wave interaction between the two spin-up fermions in two-component Fermi gases is responsible to the discrepancy. Meanwhile, it is noted that the

scaling behavior could be strongly influenced by the unitary behavior [25, 26] as well as the finite-range effect [20, 27]. These considerations raise the interesting question of whether the predicted scaling in Ref. [24] exists only in a limit range of a .

From the experimental viewpoint, testing the scaling law using the ${}^6\text{Li}$ narrow Feshbach resonance has both advantages and disadvantages compared to the broad resonance. The first advantage is that a can be tuned from minus infinity all the way to the zero in the BCS side of the narrow resonance, providing a wide tuning range to avoid the unitary behavior. It is predicted that the scaling law on $|a|$ is only valid when the system is in the threshold regime $|a| < a_c$ [28], where $a_c = 2\hbar^2/(3m|r_{eff}|k_B T)$. m is the atomic mass, r_{eff} is the effect range of the resonance, \hbar is the Planck constant, and k_B is the Boltzmann constant. At a temperature of a few micro-Kelvin, a_c is about one thousand Bohr radius a_0 for ${}^6\text{Li}$, while the background scattering length is about $-1405 a_0$ in the broad Feshbach resonance, so it is difficult to obtain the regime of $|a| < a_c$ [29]. Second, three-body recombination is the dominant mechanism for atom loss near the narrow Feshbach resonance [30], providing a more obvious way to determine the three-body loss rate. For disadvantage, the scaling law in the narrow Feshbach resonance is affected by the finite-range effect. Previous theoretical predictions of the scaling have been limited to the regime $|a| > r_{vdw}$, where r_{vdw} denotes the range of the van de Waals potential. If $|a| > r_{vdw}$ is not well satisfied, the finite-range effect must be included in the scaling models [31–33].

In this letter, we report the precision measurement of the three-body atomic loss rate L_3 for an ultracold two-component ${}^6\text{Li}$ Fermi gas near its narrow s -wave Feshbach resonance. We first confirm that the threshold behavior of $L_3 \propto T$ is valid in the narrow s -wave Feshbach resonance and covers an extremely large range as long as the system is

away from the unitary regime $|a| > a_c$. We then study L_3 in the intermediate interacting regime $r_{vdw} < |a| < a_c$, and find that $L_3 \propto |a|^{2.60(5)}$. Moreover, due to the finite range effect, a correction of $|a|^{5.9(15)}/|L_e|^{3.3(10)}$ is obtained when $|a|$ closes to a_c . Here $L_e = (1/2r_{eff}a^2)^{1/3}$ is an effective scattering length including both a and r_{eff} [34, 35]. This correction becomes larger as $|a|$ increases. For the data near the zero crossing $|a| < r_{vdw}$, we find that the scaling behavior $L_3 \propto (|a|^{2.60(5)} + L_e^{2.58(4)})$, such correction of $L_e^{2.58(4)}$ becomes larger with decreasing $|a|$. In the zero-crossing limit, the scaling dependence only on L_e . With a correction factor, we find that the value of L_e closes to r_{vdw} , which is consistent with the fact that the only length scale in the zero-crossing limit is r_{vdw} .

The two lowest hyperfine ground states mixed ${}^6\text{Li}$ Fermi gas are loaded into a crossed-beam optical dipole trap. The gas temperature is lowered through a force evaporative cooling at a magnetic field of 300 G with a balanced spin. After cooling, the gas temperature is tuned by changing the final trap depth with an atom number of about 2×10^5 per spin. We also adjust the ratio between the trap depth and the gas temperature so that the reduced temperatures T/T_F are maintained around one and thus the gas can be treated as thermal. Here T_F is the gas Fermi temperature.

The experimental procedure for the three-body atomic loss measurement is as follows. First, the magnetic field is rapidly-swept over the narrow resonance to 570 G and held for a 100 ms to rethermalize the gas. Second, the magnetic field is precisely tuned in about 50 ms to the target field at which the three-body loss occurs [36]. The target field is above the resonance $B_0 = 543.2704(16)$ G in the range of 10 to 100 mG, comparable to the resonance width $\Delta=0.1$ G. The stability of our magnetic field is controlled to 1.6 mG [37], and the gas is remains in the target field for a variable time of about 50 ms \sim 450 ms. After the three-body interaction in the target field, the magnetic field is rapidly returned to 570 G within 5 ms for taking the time-of-flight absorption imaging.

We follow the procedure in Ref. [30] to attract the L_3 through the time-dependent atom number $N(t)$ with the three-body loss rate differential equation: $\dot{N}(t) = -L_3V^{-2}N^3(t)$, where $V = (2\sqrt{3}\pi)^{3/2}\sigma_x\sigma_y\sigma_z$ and $\sigma_{x,y,z}$ denotes the Gaussian widths. In the experiments, $\sigma_{x,y,z}$ are also recorded with the absorption imaging.

We measure L_3 in a wide range of magnetic field detuning $\Delta B = B - B_0$ at various gas temperatures from 0.56 μK to 3.13 μK . The results are shown in Fig. 1 a). Here, ΔB is converted to $|a|$ by a theory formula $a(B) = a_{bg}(1 - \Delta/\Delta B)$ with a background scattering length $a_{bg} = 59 a_0$. In the thermal regime, $L_3(T)$ has a threshold behavior of $L_3 \propto T$ given by the theoretical averaging of the three-body recombination rate $K_3(E)$ over the collision energy E with a Maxwell-Boltzmann distribution. Figure 1 b) shows the fit of the magnetic field dependence of the threshold behavior $L_3 \propto T^\lambda$, where λ is a free parameter. It is found that λ equals to -2 at resonance, which agrees with the prediction [28], and it

starts to increase and reaches the value of one (blue horizontal line) until $\Delta B = 0.04$ G. Below this value, the unitary behavior significantly affects the scaling. We verify this conclusion by refitting the data with a narrower temperature range in the Supplementary Materials (SM), which shows λ equals to one in a range of $0.02 \text{ G} < \Delta B < 0.12 \text{ G}$. Therefore, we conclude that the threshold behavior $L_3 \propto T$ is not only valid in the intermediate interacting regime but also in the weakly interacting regime. Figure 1 c) shows a plot of L_3 as a function of T when $\Delta B = 0.04$ G, 0.045 G, and 0.05 G, respectively. They show a monotonic increase over the temperature range we studied and can be well fitted by $\ln(L_3) = \lambda \ln(T) + b$ with $\lambda = 0.89(8), 0.99(14), 0.95(13)$.

We find that the unitary effect near the resonance limits the scaling behavior, requiring $|a| < a_c$. We plot the values of a_c for different temperatures as solid lines in Fig. 1a). It can be seen that a_c decreases with increasing T_0 . So, when $T = 8.7 \mu\text{K}$, $a_c = r_{vdw} \sim 31a_0$ (black dashed line), indicating that the intermediate interacting regime disappears. To maintain this regime, the gas temperatures in this work are kept below 3 μK , which is lower than the temperature in the previous studies of three-body recombination near the narrow resonance [30, 38]. This proper temperature range is one of the key factors to implement the measurements presented in this work.

Next, we study the scattering length scaling law. As seen in Fig. 1a), L_3 begins to increase linearly with $|a|$ when $|a| > r_{vdw}$ (black dashed line) and levels off after $|a| > a_c$ (colored solid lines) in the log-log plot. In the intermediate regime $r_{vdw} < |a| < a_c$ (filled symbols), L_3 shows scaling law dependence of $|a|$. We normalize L_3 by $k_B T$ and plot it as a function of $|a|$ in Fig. 1d). Due to the three-body heating, the measured magnetic field dependence of the gas temperature is used to correct the data, which reduces some errors in the fits of Figs. 1b-d) (more details at SM). Note that all data in the intermediate interacting regime collapse to a single linear line. We fit the data in the intermediate interacting regime with

$$L_3(a) = C \frac{k_B}{\hbar} T |a|^\xi, \quad (1)$$

and the best-fit results is $\xi = 2.60(5)$ with $C = 6.28(146) \times 10^{-46}$. This result is close to the prediction of the zero-range model for three-body recombination in two-component Fermi mixtures, $|a|^{2.455}$ in the BCS side of the Feshbach resonance rather than $|a|^6$ in the BEC side due to the three-body repulsive effective potential [24, 28].

Beyond the intermediate interacting regime, Figure 1 d) shows discrepancies from the $|a|^{2.60}$ scaling on both sides. To investigate these discrepancies, we introduce the effective scattering length L_e and re-plot the data in Fig. 1d) into the format of $C = \hbar L_3 / (k_B T |a|^{2.60})$ versus $|L_e/a|$, as shown in Fig. 2. Therefore, the discrepancies are significantly transferred into the deviations of parameter C with a larger deviation appearing in the weakly interacting regime $|a| < r_{vdw}$ (vertical dashed line presents the $|L_e/r_{vdw}|$) and

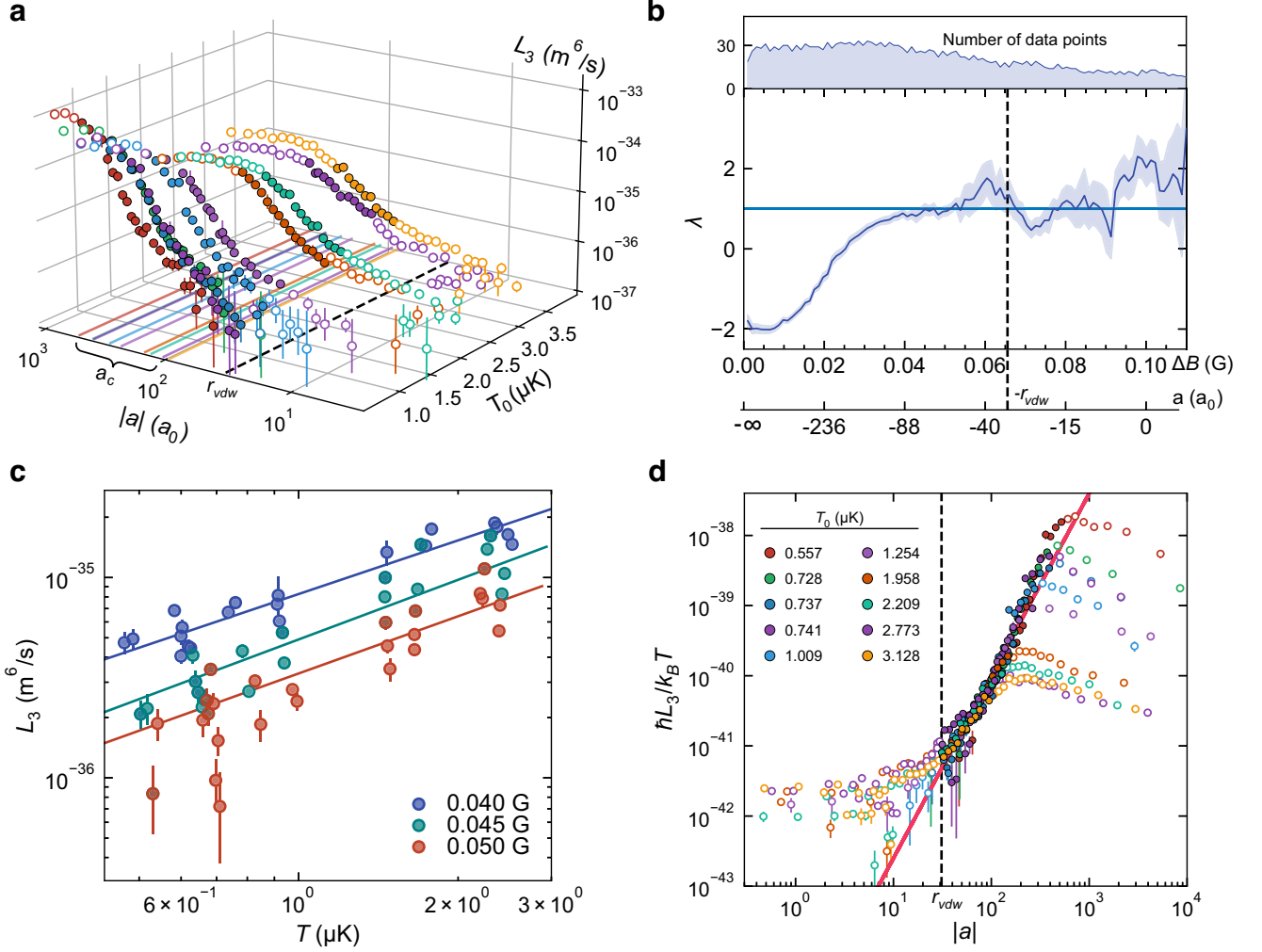


FIG. 1. a) 3D plot of L_3 vs $|a|$ and initial temperature T_0 . Colored solid lines denote the values of a_c for different temperatures. b) plot of λ vs ΔB . Horizontal blue line indicates the $\lambda = 1$. The light shadow shows the standard deviation of the fitting, and it becomes larger when fewer data points are used. c) L_3 versus T at $\Delta B = 0.04$ G (blue), 0.045 G (cyan), and 0.05 G (red). Solid lines are their best-fitting. d) normalized three-body loss rate $\hbar L_3/k_B T$ vs $|a|$. Red line is the fitting of $L_3 \propto |a|^{2.60(5)}$. In these figures, filled symbols are the data within an intermediate interacting regime, and the black dashed lines are the r_{vdw} or the ΔB has a corresponding value of $|a| = r_{vdw}$. Vertical error bars in these figures are the standard derivations.

another smaller deviation in the stronger interacting regime $2 < |L_e/a| < 5.5$. It is known that C remains constant in three-body recombination as long as the coupling strength between the quasi-bound and the deeper bound molecular states follows the same threshold and scaling behavior [20]. Here, the deviations from C are assumed as the consequence of finite-range effects and expressed with a correction of the L_3 in terms of L_e/a . The baseline of Fig. 2 equals the fitted value of Fig. 1d). The linearly increasing deviations in the log-log plot suggest power-law dependencies of L_e/a . We fit the data with $C = C_0[1 + |\beta_1 L_e/a|^{\gamma_1} + |\beta_2 L_e/a|^{-\gamma_2}]$ and obtain a best-fit result of $\beta_1 = 0.044(1)$, $\gamma_1 = 2.58(4)$, $\beta_2 = 0.23(2)$,

and $\gamma_2 = 3.3(10)$.

In the weakly interacting regime, because $|\beta_1 L_e/a|^{\gamma_1}$ dominates the scaling, the scaling law approximates as

$$L_3(a, L_e) = C_0 \frac{k_B T}{\hbar} (1 + |\beta_1 L_e/a|^{\gamma_1}) |a|^\xi. \quad (2)$$

When $a \rightarrow 0$ and $\xi = 2.60 \approx \gamma_1 = 2.58$, the scaling law is further simplified as a single dependence on L_e as $L_3 = C_0 (k_B T/\hbar) |\beta_1 L_e|^{\gamma_1}$. These scaling changes are also evident by analyzing the values of $|a|$, L_e , and $\beta_1 L_e$. As shown in Fig. 3, $|\beta_1 L_e| > |a|$ when $|a| < r_{vdw}$. We noted that the same conclusion has also been found in the s -wave

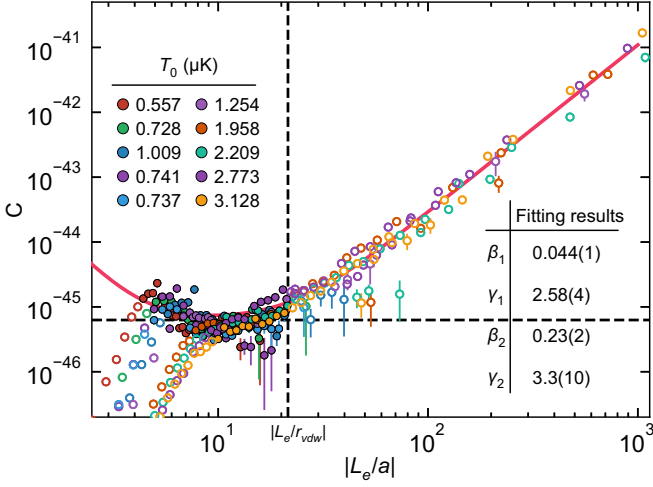


FIG. 2. Parameter C versus $|L_e/a|$. Black line presents the baseline with an averaged value of $C_0 = 6.28 \times 10^{-46}$ in the range of $5.5 < L_e/|a| < 20$. Filled symbols are the data in the intermediate interacting regime. Red line displays the best-fitting of $C = C_0(1 + |\beta_1 L_e/a|^{\gamma_1} + |\beta_2 L_e/a|^{-\gamma_2})$ with a fixed C_0 and the fitted $\beta_1 = 0.044(1)$, $\gamma_1 = 2.58(4)$, $\beta_2 = 0.23(2)$, and $\gamma_2 = 3.3(10)$.

three-body boson systems [35], where L_e replaces a as the length scale and coordinates the scaling behavior. Different from their experiments in the bosonic systems, a coefficient of β_1 is obtained from our fitting. We should emphasize that β_1 plays an important role in our data analysis. It also makes $\beta_1 L_e$ roughly equals r_{vdw} , which is the single length scale when $a = 0$.

L_e is energy-independent so that it maintains the threshold law of $L_3 \propto T$ in the weakly interacting regime. And it will be different if other possible length scales, like $L_e^3 k^2$, and $a(k) = a + L_e^3 k^2$ (k denotes the wavenumber of collision energy E), are used. Furthermore, since the measured L_3 does not vanish in the weakly interacting regime, even when $a = 0$ [30, 38], so neither a , nor $a(E) = a + L_e^3 k^2$, nor $a + \beta_1 L_e$ can be used to describe the scaling due to their zero-crossing in the weakly interacting regime when $T \sim 1\mu\text{K}$ (more details at SM). Therefore, we suggest that L_e is the universal length at weakly interacting for the presented work. Further tests using two-component s -wave boson systems and other fermionic systems could be implemented to test this suggestion.

In the stronger interacting regime, the $|\beta_1 L_e|^{\gamma_1}$ can be ignored, and the scaling becomes

$$L_3(a, L_e) = C_0 \frac{k_B T}{\hbar} (1 + |\beta_2 \frac{L_e}{a}|^{-\gamma_2}) |a|^{\xi}. \quad (3)$$

As shown in Eq. 3, the finite-range correction of $|\beta_2 L_e/a|^{-\gamma_2}$ accomplishes the original $|a|^{2.60}$ scaling, when $a \sim a_c$. So, in Eq 3, there are two terms related to $|a|$, which are the $|a|^{2.60(5)}$ scaling and the $|a|^{3.3(10)+2.60(5)=5.9(15)}$ scaling. This is different from the scaling in the weakly interacting case. The experiment in the spin-polarized gas of ^6Li atoms near a p -wave Feshbach resonant recently also supports two scaling behav-

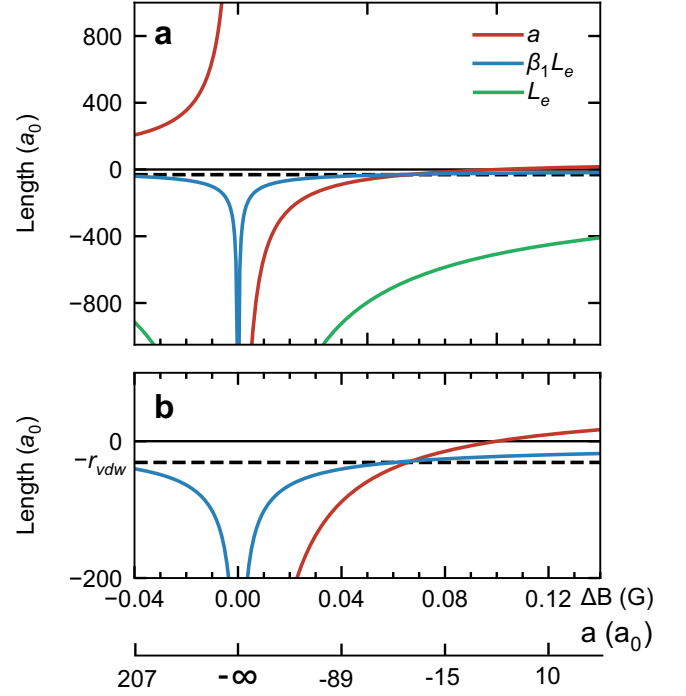


FIG. 3. a) a (red), L_e (green), and $\beta_1 L_e$ (blue) versus ΔB near the narrow Feshbach resonance. b) A zoom-in figure on the vertical axis. Black dashed lines present r_{vdw} . $\beta_1 L_e$ shows a low change when $\Delta B > 0.04$ G and roughly equals to r_{vdw} . a cross with $\beta_1 L_e$ at r_{vdw} .

iors [20], where the finite-range correction increases as interaction increases. Both our s -wave experiment and their p -wave experiment show that finite-range correction of the three-body recombination has yet to be understood, expecting more experimental and theoretical studies in the future.

In summary, we have experimentally investigated the scaling law of the three-body loss rate of a two-component ^6Li Fermi gas near its narrow s -wave Feshbach resonance, in which both the threshold behavior due to the unitary limit and the finite range effect are characterized. We confirm that the threshold behavior of $L_3 \propto T$ shown for the broad resonance is also not only valid for the narrow Feshbach resonance but also can be extended to the weakly interacting regime. In the intermediate interacting strength regime, we have identified a scaling law of $L_3 \propto |a|^{2.60}$, which is close to the theoretical prediction of $|a|^{2.455}$, but with some deviation near the threshold regime around a_c . In the weakly interacting regime, we observe a large finite-range correction and obtain a scaling of $L_3 \propto L_e^{2.58}$ with an effective scattering length L_e . Additionally, we also observe another finite-range correction in the stronger interacting region, where the original scaling of $|a|^{2.60}$ always accompanies a smaller correction of $\propto |a|^{5.9}/|L_e|^{3.3}$.

Since the unitary behavior is found to be dominant and changes the scaling law completely when $|a| > a_c$, we believe that Ref. [23] shows a $|a|^{0.79(14)}$ scaling near the broad Fes-

hbach resonance of the two-component ${}^6\text{Li}$ -Fermi gas, which could be a consequence of the unitary effect [29]. To verify this conjecture, we fit our data with a broader range of interaction strengths using the data from $r_{vdw} < |a|$ in Fig. 1d) and obtain a scaling of $\propto |a|^{0.73(8)}$. Thus, we believe that the large background scattering length near the broad Feshbach resonance messes up the original scaling of the three-body recombination.

Acknowledgments We thank Dr. Zhenhua Yu and Dr. Yangqian Yan for the helpful discussions. This work receives support from the National Natural Science Foundation of China under Grant No.12174458, 11804406, and 11774436, and from the Key-Area Research and Development Program of Guangdong Province under Grant No. 2019B030330001. The Fundamental Research Funds for the Central Universities, Sun Yat-sen University under Grant No. 2021qntd28. LL thank the supports from Guangdong Province Youth Talent Program under Grant No.2017GC010656.

* lijiam29@mail.sysu.edu.cn

† luole5@mail.sysu.edu.cn

- [1] J. P. Cox, Theory of Stellar Pulsation, *Princeton University Press* (1980).
- [2] B. Muller, Physics of the quark-gluon plasma, *nucl-th/9211010* (1992).
- [3] M. Greiner, C. A. Regal, and D. S. Jin, Emergence of a molecular Bose-Einstein condensate from a Fermi gas, *Nature* **426**, 537-540 (2003).
- [4] S. Jochim, M. Bartenstein, A. Altmeyer, G. Hendl, S. Riedl, C. Chin, J. H. Denschlag, and R. Grimm, Bose-Einstein Condensation of Molecules, *Science* **302**, 2101-2103 (2003).
- [5] T. Bourdel, L. Khaykovich, J. Cubizolles, J. Zhang, F. Chevy, M. Teichmann, L. Tarruell, S. J. J. M. F. Kokkelmans, and C. Salomon, Experimental Study of the BEC-BCS Crossover Region in Lithium 6, *Phys. Rev. Lett.* **93**, 050401 (2004).
- [6] T. Kraemer, M. Mark, P. Waldburger, J. G. Danzl, C. Chin, B. Engeser, A. D. Lange, K. Pilch, A. Jaakkola, H.-C. Nagerl, and R. Grimm, Evidence for Efimov quantum states in an ultracold gas of caesium atoms, *Nature* **440**, 315-318 (2006).
- [7] S. E. Pollack, D. Dries, and R. G. Hulet, Universality in Three- and Four-Body Bound States of Ultracold Atoms, *Science* **326**, 1683-1685 (2009).
- [8] Y. Wang, and P. S. Julienne, Universal van Der Waals Physics for Three Cold Atoms near Feshbach Resonances, *Nature Phys.* **10**, 768-773 (2014).
- [9] X.-Y. Chen, M. Duda, A. Schindewolf, R. Bause, I. Bloch, and X.-Y. Luo, Suppression of Unitary Three-Body Loss in a Degenerate Bose-Fermi Mixture, *Phys. Rev. Lett.* **128**, 153401 (2022).
- [10] C. Chin, R. Grimm, P. S. Julienne, and E. Tiesinga, Feshbach resonances in ultracold gases, *Rev. Mod. Phys.* **82**, 1225 (2010).
- [11] E. Braaten, H.-W. Hammer, D. Kang, and L. Platter, Efimov Physics in Li 6 Atoms, *Phys. Rev. A* **81**, 013605 (2010).
- [12] B. S. Rem, A. T. Grier, I. Ferrier-Barbut, U. Eismann, T. Langen, N. Navon, L. Khaykovich, F. Werner, D. S. Petrov, F. Chevy, and C. Salomon, Lifetime of the Bose Gas with Resonant Interactions, *Phys. Rev. Lett.* **110**, 163202 (2013).
- [13] L. J. Wacker, N. B. Jorgensen, D. Birkmose, N. Winter, M. Mikkelsen, J. Sherson, N. Zinner, and J. J. Arlt, Universal Three-Body Physics in Ultracold KRb Mixtures, *Phys. Rev. Lett.* **117**, 163201 (2016).
- [14] J. Johansen, B. J. DeSalvo, K. Patel, and C. Chin, Testing universality of Efimov physics across broad and narrow Feshbach resonances, *Nature Physics* **13**, 731-735 (2017).
- [15] B. D. Esry, C. H. Greene, and H. Suno, Threshold laws for three-body recombination, *Phys. Rev. A* **65**, 010705 (2001).
- [16] D. M. Stamper-Kurn, M. R. Andrews, A. P. Chikkatur, S. Inouye, H.-J. Miesner, J. Stenger, and W. Ketterle, Optical Confinement of a Bose-Einstein Condensate, *Phys. Rev. Lett.* **80**, 2027 (1998).
- [17] T. Weber, J. Herbig, M. Mark, H.-C. Nagerl, and R. Grimm, Three-Body Recombination at Large Scattering Lengths in an Ultracold Atomic Gas, *Phys. Rev. Lett.* **91**, 123201 (2003).
- [18] N. Gross, Z. Shotan, S. Kokkelmans, and L. Khaykovich, Observation of Universality in Ultracold ${}^7\text{Li}$ Three-Body Recombination, *Phys. Rev. Lett.* **103**, 163202 (2009).
- [19] H. Suno, B. D. Esry, and C. H. Greene, Recombination of three ultracold fermionic atoms, *Phys. Rev. Lett.* **90**, 053202 (2003).
- [20] J. Yoshida, T. Saito, M. Waseem, K. Hattori, and T. Mukaiyama, Scaling Law for Three-Body Collisions of Identical Fermions with p -Wave Interactions, *Phys. Rev. Lett.* **120**, 133401 (2018).
- [21] D. S. Petrov, Three-body problem in Fermi gases with short-range interparticle interaction, *Phys. Rev. A* **67**, 010703(R) (2003).
- [22] Y. Ji, G. L. Schumacher, G. G. T. Assumpcao, J. Chen, J. T. Makinen, F. J. Vivanco, and N. Navon, Stability of the Repulsive Fermi Gas with Contact Interactions, *Phys. Rev. Lett.* **129**, 203402 (2022).
- [23] X. Du, Y. Zhang, and J. E. Thomas, Inelastic Collisions of a Fermi Gas in the BEC-BCS Crossover, *Phys. Rev. Lett.* **102**, 250402 (2009).
- [24] J. P. D’Incao, and B. D. Esry, Scattering Length Scaling Laws for Ultracold Three-Body Collisions, *Phys. Rev. Lett.* **94**, 213201 (2005).
- [25] Y.-H. Chen, and C. H. Greene, P-wave Efimov physics implications at unitarity, *Phys. Rev. A* **107**, 033329 (2023).
- [26] J. P. D’Incao, C. H. Greene, and B. D. Esry, The Short-Range Three-Body Phase and Other Issues Impacting the Observation of Efimov Physics in Ultracold Quantum Gases, *J. Phys. B* **42**, 044016 (2009).
- [27] T.-L. Ho, X. Cui, and W. Li, Alternative Route to Strong Interaction: Narrow Feshbach Resonance, *Phys. Rev. Lett.* **108**, 250401 (2012).
- [28] J. P. D’Incao, Few-body physics in resonantly interacting ultracold quantum gases, *J. Phys. B* **51**, 043001 (2018).
- [29] The background scattering length of the broad Feshbach resonance of ${}^6\text{Li}$ near 832 G is $-1405a_0$. The estimated value of $a_c = \sqrt{2\hbar^2/3mk_B(T = 6\mu\text{K})} \approx 1800a_0$ is too small to be achieved near this broad Feshbach resonance..
- [30] J. Li, J. Liu, L. Luo, and B. Gao, Three-Body Recombination near a Narrow Feshbach Resonance in ${}^6\text{Li}$, *Phys. Rev. Lett.* **120**, 193402 (2018).
- [31] D. S. Petrov, Three-Boson Problem near a Narrow Feshbach Resonance, *Phys. Rev. Lett.* **93**, 143201 (2004).
- [32] E. Braaten, and H.-W. Hammer, Universality in few-body systems with large scattering length, *Physics Reports* **428**, 259-390 (2006).
- [33] Y. Wang, J. P. D’Incao, and B. D. Esry, Ultracold three-body collisions near narrow Feshbach resonances, *Phys. Rev. A* **83**, 042710 (2011).
- [34] C. L. Blackley, P. S. Julienne, and J. M. Hutson, Effective-range approximations for resonant scattering of cold atoms, *Phys. Rev. A* **89**, 042701 (2014).

- [35] Z. Shotan, O. Machtey, S. Kokkelmans, and L. Khaykovich, Three-Body Recombination at Vanishing Scattering Lengths in an Ultracold Bose Gas, *Phys. Rev. Lett.* **113**, 053202 (2014).
- [36] Y. Chen, S. Peng, H. Gong, X. Zhang, J. Li, and L. Luo, Characterization of the magnetic field through the three-body loss near a narrow Feshbach resonance, *Phys. Rev. A* **103**, 063311 (2021).
- [37] S. Peng, H. Liu, J. Li, and L. Luo, Collisional cooling of a Fermi gas with three-body recombination, *arXiv:2107.07078*.
- [38] E. L. Hazlett, Y. Zhang, R. W. Stites, and K. M. O'Hara, Realization of a Resonant Fermi Gas with a Large Effective Range, *Phys. Rev. Lett.* **108**, 045304 (2012).

SUPPLEMENTARY MATERIALS

S1: Corrections of the temperature fluctuation

We observe a magnetic field dependent temperature fluctuation $T(\Delta B)/T_0$, which is due to three-body heating or cooling [1], where T_0 stands for the initial temperature measured at a far-off resonance of a 570 G magnetic field. Figure S.1 shows a typical T as a function of the magnetic field detuning ΔB . It can be seen that the temperature fluctuation is less than 20% in the most magnetic fields.

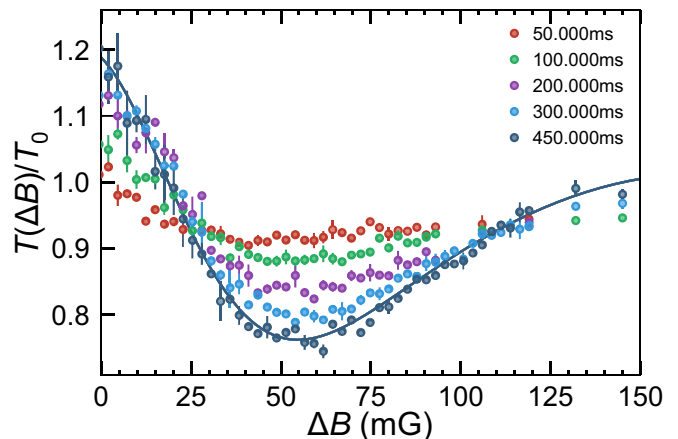


FIG. S.1. A typical T/T_0 versus ΔB for $T_0 = 3.13\mu\text{K}$. The different color present the different holding time durations. The temperature drops is due to three-body cooling of our work [1]. The solid line is a smoothing spline of the temperatures.

In Fig.1 b and c, the T^λ is obtained by fitting the L_3 at different temperatures for a given ΔB , and we use correction T instead of the initial temperature T_0 . In Fig.1 d, the correction T is also used to obtain the temperature normalized three-body atomic loss rate $\hbar L_3/k_B T$.

S2: The range of the intermediate interacting regime

The scattering length scaling law of the L_3 holds in the regime of indeterminate interacting, where $|a|$ lies between the lower limit of r_{vdw} and the upper limit of a_c . Here, a_c characterizes the condition of the unitary regime that can be determined by the ratio between the thermal energy and the quasi-molecule binding energy when $a < 0$. When the binding energy is smaller than the thermal energy, we treat the system in the unitary regime.

In a narrow Feshbach resonance, the two-body s -wave collision amplitude f has an effective-range factor r_{eff} as

$$f = -\frac{1}{a^{-1} - r_{eff}k^2/2 + ik}. \quad (\text{S.1})$$

At the pole of f , we obtain the binding energy of the molecule $E_b = \hbar^2/(2\mu a'^2)$, where $a' = r_{eff}/(-\sqrt{-1 + 2r_{eff}/a} + i)$

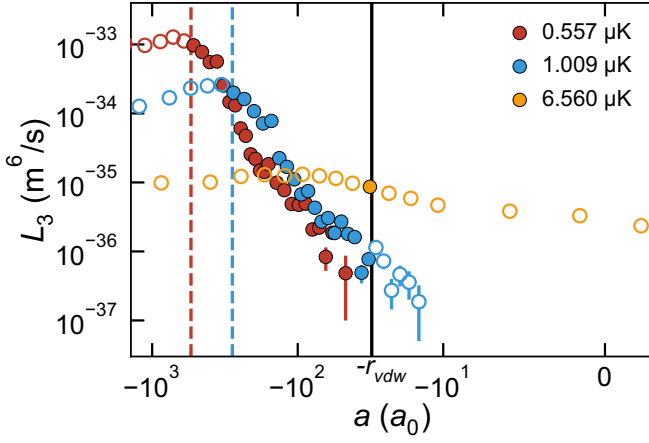


FIG. S.2. L_3 as a function of a at various temperatures of $0.557 \mu\text{K}$ (red), $1.009 \mu\text{K}$ (blue) and $6.560 \mu\text{K}$ (orange), respectively. Black solid line is $r_{vdw} = 31a_0$. Colored dashed lines present their a_c . The filled symbols between $r_{vdw} < |a| < a_c$ are the data in the intermediate interacting regime, where we use to obtain the scaling law. For the orange data, the range of intermediate interacting regime almost vanishes.

and μ is the reduced mass of two-body system. We approach $E_b = \hbar^2/(\mu r_{eff}a)$ when $r_{eff} \gg a$. Since the gas temperatures are around $T/T_F \sim 1$, we use $3k_B T$ to the averaged thermal energy of a trapped atom. When $E_b = 3k_B T$, we obtain $a_c = 2\hbar^2/(3m|r_{eff}|k_B T)$.

Figure S.2 shows L_3 at different temperatures. For the red and blue data (low temperatures), L_3 decreases when a approach the resonance point, we label the a_c as the red and blue dashed lines. It can be seen that the turning point is around a_c . But for orange data (high temperature), the decreasing is not obvious. These data show a_c decrease as T increase. When $a_c = r_{vdw}$, $T = 8.7 \mu\text{K}$, then the intermediate interacting regime vanishes. This indicate that, to obtain the scaling law in the intermediate interacting regime, we should use the gas temperature T well below $8.7 \mu\text{K}$.

S3: Threshold behavior near the resonant

In the main text, we state that the fitted λ in Fig.1 b) deviates from one when the magnetic field is closed to the resonant. In this section, we provide more details.

We obtain the λ by fitting the L_3 with a power law of T^λ at a given magnetic field detuning ΔB . The data in $\Delta B \pm 3.5$ mG are binned to the data of ΔB because of the magnetic field fluctuation. The blue curve in Fig. S.3 shows the result of λ from $0.56 \mu\text{K}$ to $3.13 \mu\text{K}$. Then, we choose the data in a narrow range of temperature, $T < 2\hbar^2/(3mk_B r_{eff}a)$, to draw the red curve. The reason is that when $T > 2\hbar^2/(3mk_B r_{eff}a)$, the data are in the unitary regime as we described in the main text. Figure S.3 shows that by redrawing the data in a narrower range (red curve), λ re-

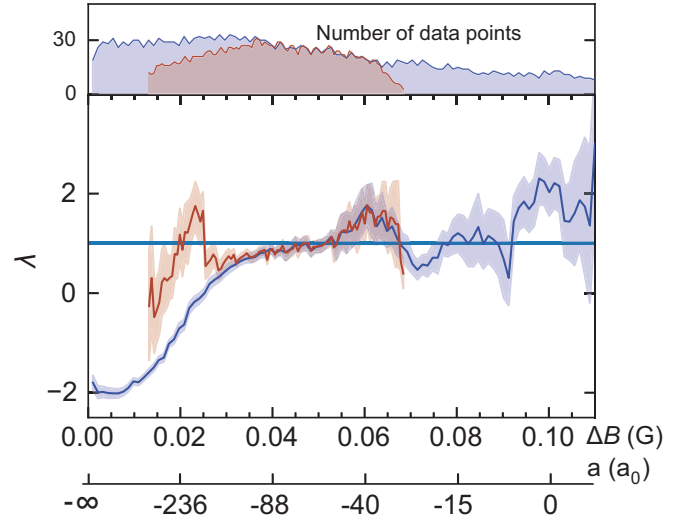


FIG. S.3. The fitted λ with all temperature data (blue curve) and chosen low temperature data (red curve). Top panel displays the number of temperature points used in two fits. The horizontal line presents $\lambda = 1$, and the light shadows are the standard derivation of the fittings.

turns to one in the regime of $0.015 \text{ G} < \Delta B < 0.04 \text{ G}$. Thus, the divergence of the blue curve in the above regime is because some high temperature data are beyond the intermediate interacting regime. When $\Delta B < 0.015 \text{ G}$, the temperature range of the intermediate interacting regime decrease, meaning we need very low temperature data to draw the red curve. Limited by our experiment, it is difficult to generate a very low temperature data to satisfy the condition of the intermediate interacting regime. So, the red curve stops around 0.015 G .

S4: Energy dependence of scattering length: effective scattering length L_e

The two-body scattering length of the narrow s -wave Feshbach resonance of ${}^6\text{Li}$ can be approximated as

$$a = a_{bg} \left(1 - \frac{\Delta}{\Delta B}\right), \quad (\text{S.2})$$

where resonance width $\Delta = 0.1 \text{ G}$, background scattering length $a_{bg} = 59 a_0$, and resonance center $B_0 = 543.2704 \text{ G}$. In a thermal gas, the collision energy $E = \hbar^2 k^2 / 2\mu$, and the low-energy effective expansion of a is

$$a(E) = a + \frac{1}{2} r_{eff} a^2 k^2. \quad (\text{S.3})$$

Here, the value of the effective collision length $L_e = (r_{eff} a^2 / 2)^{1/3}$ is taken from Ref. [2], where it is obtained by a coupled channel calculation. For more convenient, we use its parabolic approximation given by Ref. [2] for ${}^6\text{Li}$ narrow s -wave Feshbach resonance as

$$r_{eff} a^2 = v + r_0 (a - a_{ext})^2, \quad (\text{S.4})$$

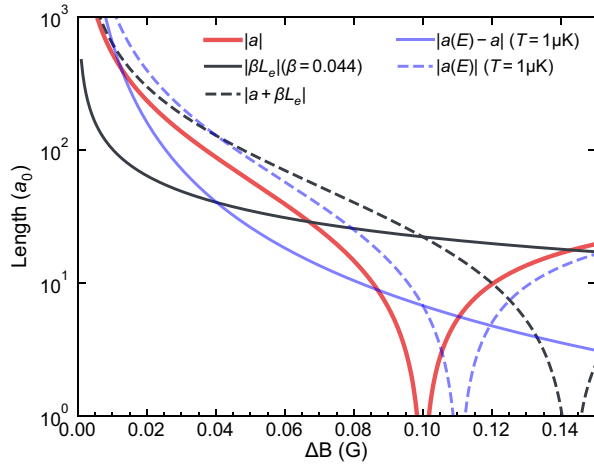


FIG. S.4. Several typical effective scattering lengths versus ΔB . k_T is the thermal wave number. a is the two-body s -wave scattering length. βL_e is the scaled used in our experiment and Ref.18 in the main text. $a(E)$, $(a + \beta L_e)$ and $[a(E) - a]$ are the other possible candidates for the length scale.

to calculate the value of L_e , where $v = -4.9 \times 10^6 a_0^3$, $r_0 = -71000 a_0$, and $a_{ext} = 60 a_0$. The effective collision length is important in studying the finite-range corrections of the scaling law. Especially, the measured L_3 does not vanish as a at the zero-crossing.

Figure S.4 plots several candidates for the new length scales. It can be seen that L_e and its reduced value βL_e keeps finite at $a = 0$ and other length scales show a zero-crossing near $a = 0$. This indicates that for $a = 0$, L_e and βL_e could be a nonzero length scale to describe the behavior of the systems.

S5: Experimental details

The experiment parameters, contain trapping frequencies $\omega_{x,y,z}$, initial atom number N_0 , Fermi temperature T_F , and reduced temperature T_0/T_F , of our data at different temperatures are listed in Tab. I.

S7: Raw Data

TABLE I. Summary of $\omega_{x,y,z}$, N_0 , T_F and T_0/T_F at various temperatures T_0 .

T_0 (μ K)	ω_x (Hz)	ω_y (Hz)	ω_z (Hz)	N_0	T_F (μ K)	T_0/T_F
0.557	2281.9	2282.9	203.1	1.25×10^5	0.71	0.79
0.728	2791.9	2797.5	264.7	1.60×10^5	0.96	0.76
0.737	2629.2	2638.9	261.4	2.10×10^5	1.01	0.73
0.741	2459.4	2468.5	244.5	2.02×10^5	0.93	0.80
1.009	3221.4	3231.5	314.1	1.85×10^5	1.17	0.86
1.254	3718.3	3731.9	369.7	3.00×10^5	1.60	0.78
1.958	4157.2	4172.4	413.4	2.92×10^5	1.78	1.10
2.210	4554.0	4570.7	452.8	3.05×10^5	1.97	1.12
2.773	5258.5	5277.8	522.9	3.00×10^5	2.27	1.22
3.128	4918.8	4936.9	489.1	3.22×10^5	2.17	1.44

TABLE II: Raw data in the main text.

T_0 (μ K)	ΔB (mGs)	$L_3(\times 10^{-36} \text{m}^6/\text{s})$	$\sigma(L_3)(\times 10^{-36} \text{m}^6/\text{s})$
0.557	1.09	426.198	56.563
0.557	2.39	867.059	37.868
0.557	3.69	1029.051	41.222
0.557	4.99	970.742	18.615
0.557	6.29	1101.383	53.897
0.557	7.59	1277.342	70.087
0.557	8.89	1123.803	81.089
0.557	10.19	971.887	69.768
0.557	11.49	777.339	76.364
0.557	12.79	554.508	52.861
0.557	14.10	565.887	83.862
0.557	15.40	254.082	25.367
0.557	16.70	147.089	11.723
0.557	18.00	130.951	12.178
0.557	19.30	60.697	4.435
0.557	20.60	47.342	3.742
0.557	21.90	25.530	1.613
0.557	23.20	21.920	1.238
0.557	24.50	14.833	0.788
0.557	25.80	14.148	0.899
0.557	27.10	18.405	1.585
0.557	29.71	9.920	0.562
0.557	32.31	7.728	0.753
0.557	34.91	4.878	0.522
0.557	37.51	4.729	0.600
0.557	40.11	4.936	0.562
0.557	42.72	2.082	0.324
0.557	45.32	2.218	0.383
0.557	47.92	0.833	0.311
0.557	50.52	1.868	0.338
0.557	55.73	0.484	0.384
0.728	0.69	187.000	6.870
0.728	3.29	285.000	14.000
0.728	5.89	422.000	16.200
0.728	8.49	539.000	16.500
0.728	11.09	579.000	32.200
0.728	13.70	434.000	17.100
0.728	16.30	249.000	16.400

0.728	18.90	148.000	8.670	0.741	44.35	2.447	0.314
0.728	21.50	80.200	6.160	0.741	46.96	3.476	0.242
0.728	22.80	59.800	4.740	0.741	49.56	0.971	0.270
0.728	24.10	44.500	3.470	0.741	52.16	0.720	0.344
0.728	25.40	28.400	1.650	0.741	57.36	0.319	0.273
0.728	26.70	19.900	0.957	0.741	59.96	0.290	0.222
0.728	28.01	13.800	0.760	0.741	67.77	1.059	0.183
0.728	29.31	13.100	0.507	1.009	1.99	29.756	4.964
0.728	30.61	10.100	0.664	1.009	4.59	126.854	3.290
0.728	31.91	7.390	0.553	1.009	7.19	168.431	6.678
0.728	33.21	8.910	0.524	1.009	9.79	232.641	5.401
0.728	34.51	6.810	0.560	1.009	12.39	251.577	10.508
0.728	35.81	7.050	0.593	1.009	15.00	262.024	15.960
0.728	37.11	6.840	0.368	1.009	17.60	199.441	9.937
0.728	39.71	5.100	0.477	1.009	20.20	161.921	9.055
0.728	44.92	4.090	0.357	1.009	22.80	107.915	8.138
0.728	50.12	1.940	0.344	1.009	25.40	71.585	2.511
0.728	52.72	2.430	0.370	1.009	28.01	77.943	4.167
0.728	55.33	0.675	0.518	1.009	30.61	22.496	1.250
0.728	70.94	0.384	0.317	1.009	33.21	16.817	0.824
0.737	0.12	67.071	4.394	1.009	35.81	11.085	0.239
0.737	2.72	135.837	3.913	1.009	38.41	6.703	0.232
0.737	5.33	218.989	12.317	1.009	41.02	7.489	0.368
0.737	7.93	278.236	9.343	1.009	43.62	4.297	0.336
0.737	10.53	343.895	8.396	1.009	46.22	2.702	0.169
0.737	13.13	277.264	10.148	1.009	48.82	3.047	0.143
0.737	15.73	221.894	6.245	1.009	51.42	1.848	0.329
0.737	18.33	145.798	6.541	1.009	54.02	2.706	0.242
0.737	20.94	83.524	9.006	1.009	56.63	1.794	0.269
0.737	23.54	44.938	1.709	1.009	59.23	1.614	0.212
0.737	26.14	20.345	1.230	1.009	61.83	0.491	0.146
0.737	28.74	11.739	0.455	1.009	64.43	0.771	0.146
0.737	31.34	8.195	0.324	1.009	67.03	1.139	0.193
0.737	33.95	7.142	0.575	1.009	69.64	0.725	0.174
0.737	36.55	4.052	0.343	1.009	72.24	0.272	0.128
0.737	39.15	4.527	0.348	1.009	74.84	0.466	0.156
0.737	41.75	3.021	0.400	1.009	77.44	0.358	0.158
0.737	44.35	2.258	0.260	1.009	80.04	0.187	0.137
0.737	46.96	2.089	0.267	1.254	0.07	42.079	2.809
0.737	49.56	2.347	0.278	1.254	1.37	65.807	5.209
0.737	52.16	1.533	0.253	1.254	2.68	75.198	4.819
0.737	54.76	1.025	0.228	1.254	7.88	119.685	7.309
0.737	57.36	0.901	0.219	1.254	13.08	130.280	3.909
0.737	59.96	0.616	0.308	1.254	18.29	120.530	6.543
0.737	62.57	0.470	0.158	1.254	23.49	76.989	3.499
0.737	70.37	0.400	0.259	1.254	26.09	59.935	11.637
0.741	0.12	93.953	7.041	1.254	27.39	42.476	2.640
0.741	2.72	142.917	5.608	1.254	28.69	38.028	2.651
0.741	5.33	211.228	7.591	1.254	30.00	29.562	1.877
0.741	7.93	287.682	9.142	1.254	32.60	20.758	1.115
0.741	10.53	426.035	12.220	1.254	33.90	18.786	1.459
0.741	13.13	395.941	6.968	1.254	35.20	14.613	1.150
0.741	15.73	328.559	13.895	1.254	37.80	7.363	0.521
0.741	18.33	194.277	4.761	1.254	39.10	8.142	1.914
0.741	20.94	162.876	7.737	1.254	40.40	6.058	0.375
0.741	23.54	60.176	3.071	1.254	43.00	5.306	0.248
0.741	26.14	31.264	1.737	1.254	44.31	3.744	0.243
0.741	28.74	15.701	0.879	1.254	49.51	2.758	0.098
0.741	31.34	14.801	2.276	1.254	52.11	2.410	0.234
0.741	33.95	7.775	0.429	1.254	54.71	1.797	0.144
0.741	36.55	5.630	0.494	1.254	59.92	1.628	0.148
0.741	39.15	4.450	0.238	1.254	65.12	1.501	0.122
0.741	41.75	2.670	0.281	1.254	70.32	1.073	0.062

1.254	75.53	0.831	0.104	2.210	39.37	14.388	0.304
1.254	78.13	0.471	0.087	2.210	41.97	14.592	0.652
1.254	80.73	0.402	0.126	2.210	44.58	8.739	0.167
1.254	85.93	0.485	0.068	2.210	47.18	6.804	0.188
1.254	101.55	0.243	0.057	2.210	49.78	5.191	0.098
1.254	104.15	0.269	0.109	2.210	52.38	4.360	0.137
1.254	117.16	0.205	0.106	2.210	54.98	4.565	0.199
1.958	2.54	24.521	1.453	2.210	57.58	2.782	0.065
1.958	5.14	30.675	1.498	2.210	60.19	2.203	0.082
1.958	7.74	33.620	1.084	2.210	62.79	2.013	0.065
1.958	10.34	41.230	1.354	2.210	65.39	1.819	0.088
1.958	12.95	49.369	2.159	2.210	67.99	1.722	0.087
1.958	15.55	50.008	1.182	2.210	70.59	1.355	0.062
1.958	18.15	54.650	1.050	2.210	73.20	1.318	0.085
1.958	20.75	52.578	0.625	2.210	75.80	1.160	0.055
1.958	23.35	51.163	1.116	2.210	78.40	0.968	0.052
1.958	25.96	39.892	1.794	2.210	81.00	0.999	0.069
1.958	28.56	40.001	0.916	2.210	83.60	0.727	0.057
1.958	31.16	31.911	1.079	2.210	86.20	0.683	0.028
1.958	33.76	25.576	1.077	2.210	88.81	0.600	0.055
1.958	36.36	19.103	1.190	2.210	91.41	0.500	0.040
1.958	38.96	13.369	1.910	2.210	94.01	0.657	0.043
1.958	41.57	9.997	0.621	2.210	96.61	0.507	0.034
1.958	44.17	8.005	0.508	2.210	99.21	0.264	0.045
1.958	46.77	5.963	0.479	2.210	101.82	0.263	0.031
1.958	49.37	4.556	0.353	2.210	104.42	0.273	0.043
1.958	51.97	3.498	0.464	2.210	107.02	0.295	0.037
1.958	54.58	3.091	0.189	2.210	109.62	0.279	0.042
1.958	57.18	2.328	0.164	2.210	112.22	0.055	0.034
1.958	59.78	2.269	0.257	2.210	117.43	0.141	0.035
1.958	62.38	1.868	0.131	2.210	120.03	0.153	0.049
1.958	64.98	1.522	0.141	2.773	1.47	14.086	0.244
1.958	67.58	2.041	0.087	2.773	4.07	18.717	0.451
1.958	70.19	1.691	0.056	2.773	6.67	20.572	0.457
1.958	72.79	1.577	0.073	2.773	9.27	23.100	0.369
1.958	75.39	1.210	0.090	2.773	11.88	29.789	0.926
1.958	77.99	1.057	0.073	2.773	13.18	29.649	0.790
1.958	80.59	1.321	0.063	2.773	15.78	32.012	0.391
1.958	83.20	1.196	0.077	2.773	18.38	33.119	0.472
1.958	85.80	0.957	0.064	2.773	20.98	34.282	0.394
1.958	88.40	1.023	0.044	2.773	23.58	29.139	0.404
1.958	91.00	0.390	0.067	2.773	27.49	34.813	0.516
1.958	93.60	0.642	0.047	2.773	30.09	30.211	0.398
1.958	96.20	0.534	0.067	2.773	32.69	28.690	0.446
1.958	98.81	0.398	0.042	2.773	35.29	26.919	0.318
1.958	101.41	0.567	0.059	2.773	37.89	17.906	1.515
1.958	104.01	0.175	0.052	2.773	39.19	18.713	0.673
1.958	117.02	0.082	0.047	2.773	41.80	16.163	0.470
2.210	0.34	14.548	0.585	2.773	44.40	13.844	0.472
2.210	2.95	12.375	1.115	2.773	47.00	11.048	0.406
2.210	5.55	24.797	0.456	2.773	49.60	7.855	0.777
2.210	8.15	28.049	0.351	2.773	53.50	8.313	0.180
2.210	10.75	32.432	0.543	2.773	56.11	7.290	0.158
2.210	13.35	34.824	0.362	2.773	58.71	5.847	0.107
2.210	15.96	31.714	0.566	2.773	61.31	4.909	0.122
2.210	18.56	38.616	0.619	2.773	63.91	4.836	0.155
2.210	21.16	40.798	0.664	2.773	66.51	3.345	0.099
2.210	23.76	37.786	0.657	2.773	67.81	2.693	0.118
2.210	26.36	35.486	0.821	2.773	70.42	2.199	0.096
2.210	28.96	34.065	1.062	2.773	73.02	1.785	0.074
2.210	31.57	26.354	0.472	2.773	75.62	1.491	0.125
2.210	34.17	21.342	0.479	2.773	79.52	1.650	0.048
2.210	36.77	17.451	0.312	2.773	82.12	1.655	0.054

2.773	84.73	1.201	0.043	3.128	53.98	5.456	0.413
2.773	87.33	1.380	0.050	3.128	56.58	3.422	0.080
2.773	89.93	0.884	0.059	3.128	59.19	2.859	0.119
2.773	92.53	1.075	0.058	3.128	61.79	2.636	0.101
2.773	93.83	0.869	0.048	3.128	64.39	2.203	0.100
2.773	96.43	0.898	0.040	3.128	66.99	1.976	0.162
2.773	99.04	0.719	0.045	3.128	69.59	1.764	0.065
2.773	101.64	0.729	0.050	3.128	72.20	1.638	0.073
2.773	105.54	0.675	0.040	3.128	74.80	1.375	0.063
2.773	108.14	0.579	0.030	3.128	77.40	1.317	0.088
2.773	110.74	0.719	0.052	3.128	80.00	1.323	0.096
2.773	113.35	0.461	0.038	3.128	82.60	1.115	0.091
2.773	115.95	0.482	0.035	3.128	85.20	1.134	0.081
2.773	118.55	0.478	0.023	3.128	87.81	0.809	0.065
2.773	119.85	0.370	0.035	3.128	90.41	0.801	0.072
2.773	122.45	0.369	0.033	3.128	93.01	0.760	0.078
3.128	1.95	16.149	0.552	3.128	95.61	1.011	0.087
3.128	4.55	25.038	1.342	3.128	98.21	0.954	0.097
3.128	7.15	28.630	1.206	3.128	100.82	0.912	0.103
3.128	9.75	31.324	1.406	3.128	103.42	0.806	0.126
3.128	12.35	34.984	1.202	3.128	106.02	0.387	0.043
3.128	14.96	31.955	1.045	3.128	108.62	0.384	0.104
3.128	17.56	36.798	1.426	3.128	111.22	0.412	0.117
3.128	20.16	37.381	2.089	3.128	113.82	0.773	0.072
3.128	22.76	35.313	1.388	3.128	116.43	0.516	0.125
3.128	25.36	31.631	1.201	3.128	119.03	0.154	0.063
3.128	27.96	33.364	1.724				
3.128	30.57	24.693	0.650				
3.128	33.17	20.735	0.662				
3.128	35.77	18.137	0.408				
3.128	38.37	14.648	0.316				
3.128	40.97	16.378	1.207				
3.128	43.58	10.473	0.291				
3.128	46.18	8.265	0.190				
3.128	48.78	7.276	0.155				
3.128	51.38	5.410	0.136				

* lijiam29@mail.sysu.edu.cn

† luole5@mail.sysu.edu.cn

- [1] S. Peng, H. Liu, J. Li, and L. Luo, Collisional cooling of a Fermi gas with three-body recombination, *arXiv:2107.07078*.
- [2] C. L. Blackley, P. S. Julienne, and M. Hutson. Effective-range approximations for resonant scattering of cold atoms, *Phys. Rev. A* **89**, 042701 (2014).